Article

Not peer-reviewed version

Heterodyne Light Source Using Two Tandem Acousto-Optic Modulators Under Bragg Diffraction Conditions

Ming-Hung Chiu * and Chao-Ching Chiu

Posted Date: 21 February 2025

doi: 10.20944/preprints202502.1740.v1

Keywords: heterodyne light source; acoustic optic modulator; Bragging diffraction, SPR sensor, phase measurement; common-path heterodyne interferometry

 doi:10.20944/preprints202502.1740.v1

Article

Heterodyne Light Source Using Two Tandem Acousto-Optic Modulators Under Bragg Diffraction Conditions

Ming-Hung Chiu * and Chao-Ching Chiu

Department of Electrical-Optical Engineering of National Formosa University

* Correspondence: mhchiu@gs.nfu.edu.tw; Tel.: +886-5-6315666

Abstract: We propose a novel heterodyne light source architecture employing two tandem acousto-optic modulators (AOM) operating under Bragg-diffraction conditions. A mirror and a half-wave plate are strategically positioned between the AOMs. By fine-tuning the angle of the mirror relative to the AOMs, only the +1st- or −1st-order light is generated, allowing the two light beams to coincide. The beat frequency is determined by the difference in modulation frequencies. In order to demonstrate the feasibility of this architecture, we use this light source in common-path heterodyne interferometry (CPHI) to measure the gold film thickness of a surface plasmon resonance (SPR) sensor. The experimental results are in good agreement with the outcomes of mathematical simulations. In addition, the heterodyne light source has two linear polarizations perpendicular to each other with a frequency difference of 10 kHz, and the utilization rate of the light source can reach 90%.

Keywords: heterodyne light source; acoustic optic modulator; Bragging diffraction; SPR sensor; phase measurement; common-path heterodyne interferometry

---

1. Introduction

Heterodyne light sources commonly used in research include Zeeman lasers [1,2], Mach–Zehnder architectures [3,4], and electro-optic modulator (EOM) architecture [5]. Among these, the Zeeman laser functions as a self-contained heterodyne light source, offering a high beat frequency but at a high cost. The heterodyne light source based on the Mach–Zehnder architecture consists of two acousto-optic modulators (AOM); however, as it lacks a common-path architecture, it is susceptible to environmental disturbances. Additionally, the 0th-order light is not used, so the utilization rate of the laser is low. The heterodyne light source based on the EOM architecture requires full-wave voltage modulation, which causes a temperature rise in the electro-optic crystal, potentially leading to phase errors due to the high voltage.

Recently, Chiu et al. [6] proposed a heterodyne light source using two AOMs connected in series. While this setup is simple to implement, the diffraction efficiency remains suboptimal because the modulators are not operated under Bragg-diffraction conditions. In order to address these shortcomings, we propose an optimized configuration with two AOMs connected in series, both operating under Bragg-diffraction conditions. Through fine-tuning of the mirror and the two AOMs to ensure that the two orthogonally polarized light beams coincide, the heterodyne interference signal is substantially enhanced and the utilization rate of the laser approaches 90%.

2. Materials and Methods

In the acousto-optic modulator (AOM) shown in Figure 1a, the Bragg diffraction conditions are derived from the triangle in Figure 1b and are expressed as [7]:

 doi:10.20944/preprints202502.1740.v1

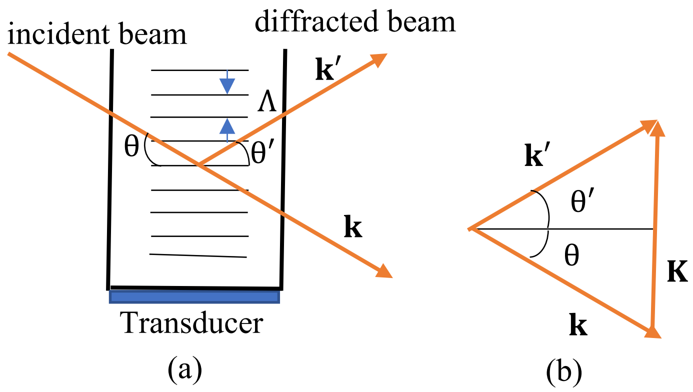

Figure 1. The +1st-order diffraction beam in acousto-optic modulator (AOM) under the Bragg diffraction condition.

$$\mathbf{k}' = \mathbf{k} + \mathbf{K}, \quad (1)$$

then $\mathrm{K} = \mathrm{k}'\sin\theta' + \mathrm{k}\sin\theta$. If $\theta' \approx \theta$ and $\mathrm{k}' \approx \mathrm{k} = \frac{2\pi}{\lambda}$, then $\mathrm{K} = \frac{2\pi}{\Lambda} = 2\mathrm{k}\sin\theta$ and:

$$\Lambda = \frac{\lambda}{2sin\theta} = \frac{v_s}{f_s} \quad (2)$$

where $\mathbf{K}$, $\mathbf{k}'$, and $\mathbf{k}$ are the wave vectors of the sound wave, diffracted beam, and incident beam, respectively, while θ and θ' are the incident and diffracted angles, respectively. Here, v_s is the sound velocity, f_s is the frequency of the sound wave or the modulation frequency, Λ is the wavelength of sound, and λ is the wavelength of the beam in the medium. If the frequency of the incident beam is $f = f_0$, then the Doppler effect causes the frequency of the diffracted beam to be $f' = f_0 - f_s$, where the beam is the +1st-order beam. Equation (2) represents the Bragg condition.

The basic optical setup of the heterodyne light source is shown in Figure 2 to further illustrate the principle of the coincidence of the two beams produced by the two AOMs connected in series. Here the modulation frequencies of AOM1 and AOM2 are f_1 and f_2, respectively. Under Bragg diffraction conditions, if the optical frequency of the laser light is f_0, then the optical frequency of the 0th-order beam from AOM1 is unchanged at f_0, while the optical frequency of the +1st-order beam is $f_0 - f_1$. The angle between these two beams is 2θ. The 0th-order beam from AOM1 is incident on the second AOM (AOM2). The optical frequency of the direct beam remains unchanged at f_0, which is denoted as beam A, while the optical frequency of the +1st-order beam is $f_0 - f_2$ and is denoted as beam A′. The angle between these two beams is 2θ. In addition, the diffracted light with a frequency of $f_0 - f_1$ is reflected into AOM2 after passing through mirror *M*. The direct light frequency remains $f_0 - f_1$, denoted as beam B, and its −1st-order beam has a frequency of $f_0 - f_1 + f_2$, denoted as beam B′. By fine-tuning the angle of mirror *M* so that the angle of incidence is θ (that is, the angle between the 0th-order beams is 2θ), the two sets of beams can coincide. One set consists of beam A′ coincident with beam B, while the other set consists of beam A coincident with beam B′. The frequency difference between the two beams in both sets is $f = |f_2 - f_1|$.

As illustrated in Figure 3, the proposed heterodyne light source consists of a laser, two AOMs (AOM1, AOM2), a mirror (M), and a half-wave plate ($W_{\lambda/2}(45°)$) positioned at an azimuth angle of 45°.

doi:10.20944/preprints202502.1740.v1

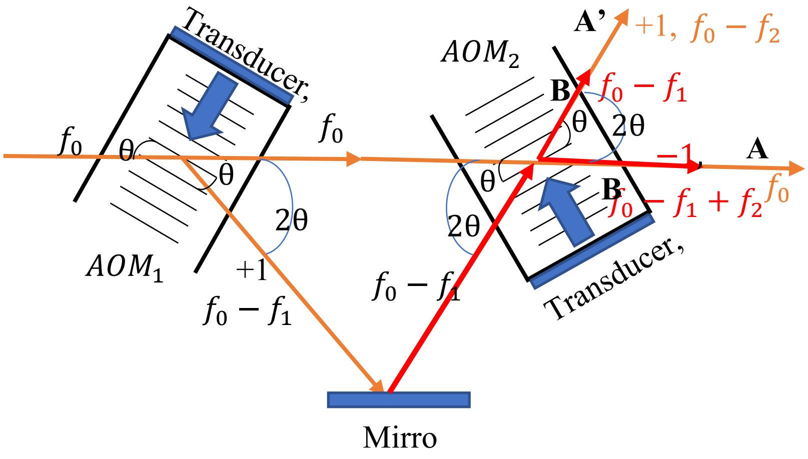

Figure 2. The basic optical setup of a heterodyne light source.

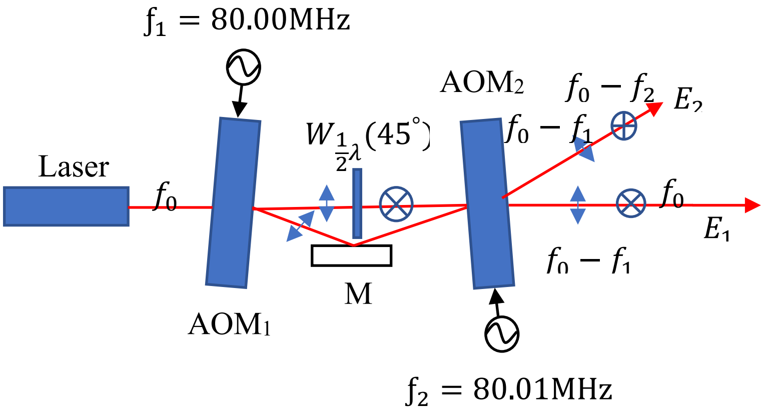

Figure 3. Schematic of the heterodyne light source utilizing two tandem AOMs in Bragg-diffraction conditions. Components: helium-neon laser (λ = 632.8 nm); AOM1, AOM2: acousto-optic modulators; $W_{\lambda/2}(45°)$: half-wave plate; M: mirror.

The acoustic waves of the two AOMs propagate in opposite directions. In this configuration, the laser operates at a frequency of f_0, and the modulation frequencies of AOM1 and AOM2 are set to f_1 (80.00 MHz) and f_2 (80.01 MHz), respectively. Fine-tuning the AOMs enables them to operate under Bragg-diffraction conditions, the diffraction efficiency of the ±1st-order light reaches approximately 44%, while the 0th-order light achieves approximately 51% efficiency. When the 0th-order light from AOM1, which is p-polarized, passes through the half-wave plate $W_{\lambda/2}(45°)$, the outgoing light becomes s-polarized, making its polarization perpendicular to that of the +1st-order light. The +1st-order light from AOM1, after being reflected by mirror M, is directed into AOM2. Upon passing through AOM2, the frequencies of the 0th- and −1st-order light beams become $f_0 - f_1$ and $f_0 - f_1 + f_2$, respectively. In addition, after the 0th-order light of AOM1 passes through AOM2, the frequencies of the 0th- and +1st-order lights from AOM2 are f_0 and $f_0 - f_2$, respectively, as illustrated in Figure 3. By adjusting the angle of mirror M relative to the AOMs, the 0th-order p-polarized light ($f_0 - f_1$) coincides with the +1st-order s-polarized light ($f_0 - f_2$), while the −1st-order p-polarized light ($f_0 - f_1 + f_2$) coincides with the 0th-order s-polarized light (f_0). The Jones vectors of the electric field intensities E_1 and E_2 can be expressed as:

$$E_1 = \begin{bmatrix} A_{x1}e^{j2\pi(f_0-f_1+f_2)t} \\ A_{y1}e^{j2\pi f_0 t} \end{bmatrix}, \tag{3}$$

And

Preprints.org (www.preprints.org) | NOT PEER-REVIEWED | Posted: 21 February 2025 doi:10.20944/preprints202502.1740.v1

$$E_2 = \begin{bmatrix} A_{x2}e^{j2\pi(f_0-f_1)t} \\ A_{y2}e^{j2\pi(f_0-f_2 t} \end{bmatrix}, \tag{4}$$

respectively, where A_{x1} and A_{y1} are the amplitudes of the electric field E_1 in the x and y directions, and A_{x2} and A_{y2} are the amplitudes of the electric field E_2 in the x and y directions, respectively. Once the two orthogonally polarized light beams coincide, two sets of heterodyne light sources are formed, with a frequency difference of $f = |f_2 - f_1| =$ 10 kHz.

3. Results

In order to demonstrate the feasibility of the proposed heterodyne light-source architecture, we use common-path heterodyne interferometry to measure the thickness of the gold film of a known surface plasmon resonance (SPR) sensor. The experimental architecture is illustrated in Figure 4.

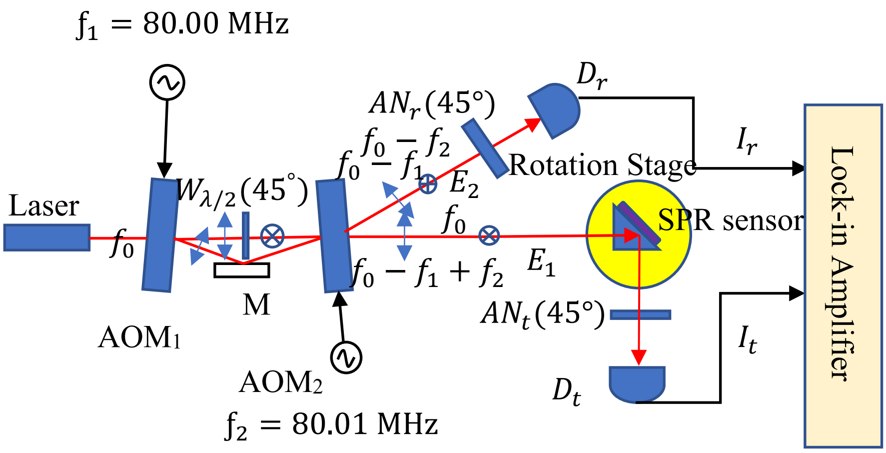

Figure 4. Verification experiment: A common-path heterodyne interferometer based on the proposed heterodyne light-source architecture used for measuring the gold-film thickness of the SPR sensor. AN_r, AN_t: analyzers; D_r, D_t: photodetectors; SPR: SPR sensor; SR830: lock-in amplifier.

We use an analyzer with a transmission axis set at a 45° angle to allow the orthogonal polarized light beams to interfere. The resulting interference signal was detected by a photodetector. The reference I_r nal detected by D_r is expressed as

$$I_r = I_{r0}(1 + V_r \; I_t \; 2\pi f t)) \tag{5}$$

and the test signal detected by D_t can be expressed as:

$$I_t = I_{t0}(1 + V_t cos(2\pi f t + \phi)), \tag{6}$$

where I_{r0} and I_{t0} are the average intensities, V_r and V_t are the visibilities, and ϕ is the phase-shift difference of the SPR sensor. The interference signals were recorded using an oscilloscope, as shown in Figure 5. According to the principle of the SPR sensor, the phase shift difference ϕ can be expressed as:

$$\phi = \delta_p - \delta_s, \tag{7}$$

where δ_p and δ_s are the phase shifts of the p- and s-polarized light beams after passing through the SPR sensor.

As illustrated in Figure 6, the refractive indices of the prism (BK7), Au, and air are denoted by $n_1, n_{2,}$, and n_3, respectively.

Preprints.org (www.preprints.org) | NOT PEER-REVIEWED | Posted: 21 February 2025 doi:10.20944/preprints202502.1740.v1

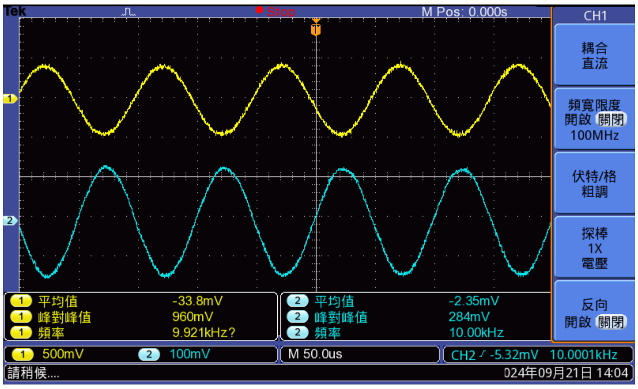

Figure 5. Wave forms of the test and reference signals. The frequency of two signals is 10kHz.

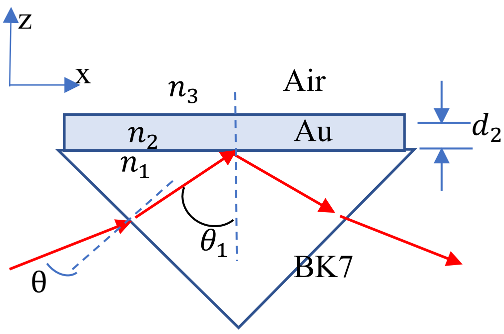

Figure 6. Configuration of SPR sensor.

The total reflection coefficient of the p- or s-polarized light can be expressed as [8]:

$$r_{123}^t = \frac{r_{12}^t + r_{23}^t e^{i2k_{z2}d_2}}{1+r_{12}^t r_{23}^t e^{i2k_{z2}d_2}} = |r_{123}^t|\angle\delta_t, t = p\ or\ s, \tag{8}$$

where d_2 is the thickness of Au and:

$$k_{z2}d_2 = k_0 n_2 d_2 cos\theta_2 = {}^{2\pi d_2}/_{\lambda_0}\,(n_2^2 - n_1^2 sin^2\theta_1)^{1/2}, \tag{9}$$

where n_2 and n_1 are the refractive indices of Au and the prism, respectively; θ_2 and θ_1 are the angles of the light beams at the Au–prism interface; $r_{ij}^t = \frac{E_i^t - E_j^t}{E_i^t + E_j^t}, (t = s\ or\ p)$ is the reflection coefficient at the boundary between mediums i and j, where $E_{i(j)}^p = {}^{n_{i(j)}{}^2}/_{k_{zi(j)}}$; $E_{i(j)}^s = k_{zi(j)}$; and $i, j = 1, 2, 3$. For a laser wavelength of 632.8 nm, the refractive indices of the BK7 prism, Au, and air are 1.51509, $(-12 + 1.26i)^{1/2}$, and 1.0003, respectively. Substituting these values into Equations (7)–(9) yields the total reflection coefficient and the phase shift difference ϕ. The resonance angle is near at 43.5° for the boundary between Au and Bk7 and surface plasmon resonance conditions must be met

$$k_{sp} = \sqrt{\frac{\varepsilon_1\varepsilon_2}{\varepsilon_1+\varepsilon_2}}\,k_0, \tag{10}$$

where ε_2 and ε_1 are the relative permittivity of Au and the Bk7 prism, respectively and k_0 is the wavenumber in vacuum.

By rotating the SPR sensor counterclockwise near the resonance angle (from 43° to 48°), the phase-shift difference ϕ and the angle of incidence θ_1 were recorded. The experimental data, denoted by red circles, are shown in Figure 7, alongside simulation results (solid line) generated using MATLAB. The optimal gold-film thickness obtained from the experiment was 35 nm, which is in good agreement with the actual gold-film thickness of the SPR sensor.

Preprints.org (www.preprints.org) | NOT PEER-REVIEWED | Posted: 21 February 2025 doi:10.20944/preprints202502.1740.v1

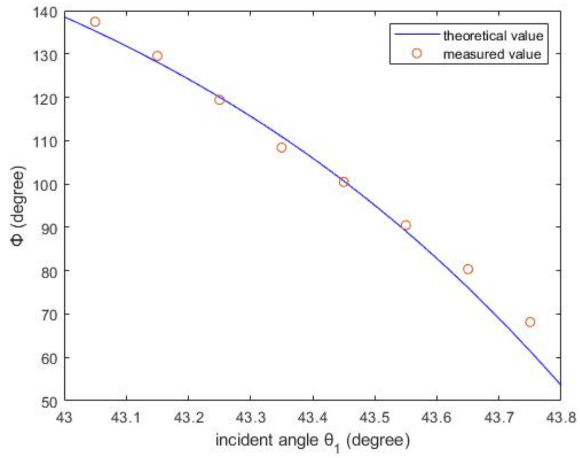

Figure 7. Experimental results for the SPR's gold-film thickness measurement using the common-path heterodyne interferometry (approximately 35 nm). Red circles: experimental values; blue line: simulation curve.

4. Discussion

These experiments confirm the feasibility of the proposed heterodyne light source as a reliable component for a common-path heterodyne interferometer. The phase resolution determined by stander deviation test was 0.04° as shown in Figure 8. From Table 1, the phase resolution of our structure is better than that of the Mach-Zehnder AOM structure and EOM architecture in our experiments. Although it is not better than Zeeman laser. But because of the low price, it still has its value. Under Bragg-diffraction conditions, the interference contrast could exceed 0.7 and the utilization rate of the light source was approximately 90%.

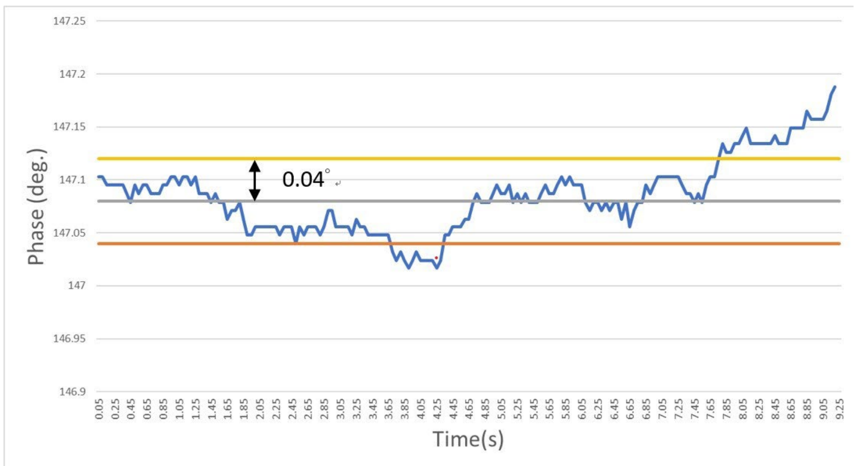

Figure 8. The standard deviation of phase measurement.

Table 1. The standard deviation of phase measurement under a general heterodyne light source.

Zeeman Laser	Mach-Zehnder structure	AOM	EOM architecture	Our structure
0.01°	0.08°		0.06°	0.04°

5. Conclusions

This heterodyne light-source architecture, featuring dual AOMs in tandem under Bragg-diffraction conditions, addresses the limitations of the Mach–Zehnder architecture regarding light-source utilization, as well as the low diffraction efficiency of previous dual-AOM architectures [6]. It offers ease of assembly and reduces the need for components such as beamsplitters, polarized beamsplitters, and an additional mirror, while only requiring the addition of a half-wave plate. This makes it a highly efficient and practical solution.

Author Contributions: Conceptualization, M.H. Chiu; methodology, M.H. Chiu; software, C.C. Chiu; formal analysis, M.H. Chiu; investigation, C.C. Chiu; resources, M.H. Chiu; data curation, C.C. Chiu; writing—original draft preparation, M.H. Chiu; writing—review and editing, M. H. Chiu; visualization, M.H. Chiu; supervision, M. H. Chiu; project administration, M.H. Chiu; funding acquisition, M.H. Chiu.

Funding. The current study was funded by the National Science and Technology Council (NSTC112-2221-E-150-035, Taiwan).

Data Availability Statement: Where no new data were created.

Acknowledgments. M.H. Chiu thanks the NSTC in Taiwan for supporting this work.

Disclosures. The authors declare no conflicts of interest.

References

1. A. S. Badger; T. A. Rabson, Zeeman effect and ruby laser polarization, *In Proceedings of the IEEE*, **1964**, *52(9),* 1047-1048. doi: 10.1109/PROC.1964.3239.
2. H. Takasaki; N. Umeda; M. Tsukiji, Stabilized transverse Zeeman laser as a new light source for optical measurement, *Appl. Opt.* **1980**, *19*, 435-441.
3. M. J. Ehrlich; L. C. Philips; J.W. Wanger, Voltage-controlled acousto-optic phase shifter, *Rev. Sci. Instrum.* **1988**, *59*, 2390-2392.
4. M. G. Gazalet; M. Ravez; F. Haine; C. Bruneel; E. Bridoux, Acousto-optic low frequency shifter, *Appl. Opt*. **1994,** *33*, 1293-1298
5. D.C. Su; M.H. Chiu; C.D. Chen, Simple two-frequency laser, *Prec. Eng*. **1996,** *18*, 161-163
6. M.H. Chiu; C.C. Chiu, Tandem heterodyne light sources with dual acousto-optic modulators as an example of the optical rotation measurement of water as a function of temperature, *Appl. Opt.* **2024,** *63*, 6955-6959. https://doi.org/10.1364/AO.531977
7. A. Yariv; P. Yeh, *Optical Waves in Crystals: Propagation and Control of Laser Radiation*, Wiley, John Wiley & son Inc.,USA, **2003**, pp.329-336.
8. H. Raether, *Surface Plasmons on Smooth and Rough Surfaces and on Gratings*, Springer Tracts in Modern Physics, Volume 111. ISBN 978-3-540-17363-2. Springer-Verlag, **1988.**